Partial oxidation of propane over Ru promoted Ni/Mg(Al)O catalysts -Self activation and prominent effect of reduction-oxidation treatment of the catalyst-

Dalin Li,[1] Masato Shiraga,[1] Ikuo Atake,[1] Tetsuya Shishido,[2] Yasunori Oumi,[1] Tsuneji Sano[1] and Katsuomi Takehira[1]*

[1]*Department of Chemistry and Chemical Engineering, Graduate School of Engineering, Hiroshima University, Kagamiyama 1-4-1, Higashi-Hiroshima 739-8527, Japan*
[2]*Department of Molecular Engineering, Graduate School of Engineering, Kyoto University, Katsura 1, Nishigyo-ku, Kyoto 615-8510, Japan*

Received 2006

*Correspondence should be addressed to:

Professor Katsuomi Takehira
Department of Chemistry and Chemical Engineering,
Graduate School of Engineering, Hiroshima University,
Kagamiyama 1-4-1, Higashi-Hiroshima, 739-8527, Japan
Phone : (+81-824)-24-6488
Telefax: (+81-824)-24-6488
E-mail: takehira@hiroshima-u.ac.jp

Abstract

Ru (0.1~0.5 wt%) loaded Ni/Mg(Al)O catalysts have been prepared by adopting the "memory effect," i.e., the reconstitution of Mg(Ni)-Al hydrotalcite from the Mg(Ni,Al)O periclase after the heat-treatment, and their catalytic activities have been tested in the partial oxidation of propane. The Ru-$Ni_{0.5}/Mg_{2.5}$(Al)O catalysts were prepared by dipping $Mg_{2.5}$(Al,$Ni_{0.5}$)O periclase derived from $Mg_{2.5}(Ni_{0.5})$-Al hydrotalcite in an aqueous solution of Ru(III) nitrate. The reconstitution of hydrotaclite took place by the "memory effect" and was simultaneously accompanied by Ru incorporation in the hydrotalcite layer, leading to the formation of the active Ni-Ru bimetal loaded catalyst after the calcination followed by the reduction. Upon O_2 purging at 700 °C during the propane partial oxidation at 600 °C, the Ru-$Ni_{0.5}/Mg_{2.5}$(Al)O catalyst showed no deactivation, while the $Ni_{0.5}/Mg_{2.5}$(Al)O catalyst was totally deactivated by the Ni oxidation. Moreover, the Ru-$Ni_{0.5}/Mg_{2.5}$(Al)O catalysts were self-activated under the reaction conditions without reduction pre-treatment with H_2. The activity of the Ru-$Ni_{0.5}/Mg_{2.5}$(Al)O catalysts was enhanced with increasing the Ru loading after the reduction-oxidation pretreatment. After the treatment, two types of Ni reduction peak were observed in the TPR of the catalysts: the 1st peak observed around 550 °C was weakened, whereas the 2nd peak observed around 750 °C was enhanced, with increasing the Ru loading. The 1st is assigned to non-active Ni^{2+} ions having square-pyramidal coordination in the outermost layer of the Mg(Al)O structure, while the 2nd is probably of active Ni-Ru bimetallic species composed of finely dispersed Ni metal particles combined with Ru.

Key Words: propane partial oxidation, H_2 production, Ru-Ni/Mg(Al)O catalyst, hydrotalcite, self activation, reduction-oxidation treatment.

1. Introduction

Hydrogen is important in oil refineries and the chemical industry and is becoming attractive as a future clean fuel for combustion engines and fuel cells [1,2]. Steam reforming of hydrocarbons, especially of CH_4, has been employed frequently as the largest and generally the most economical way to make H_2 [3]. This process has been well established and optimized over the decades; in the processes, nickel catalyst has most often been used due to its high activity and low cost [3]. Despite all this, the steam reforming process faces several drawbacks, the most significant one being the large energy input required for the endothermic reaction. Therefore, hydrogen production by the non-catalytic partial oxidation of hydrocarbons has become the second most important process. Its main advantage is that it is exothermic, but the reaction often requires very high temperature [1,2]. Consequently, the catalytic partial oxidation has received considerable attention over the past years. Research concerning the catalytic partial oxidation has been focused on CH_4, as it is believed to be still a future major feedstock for the production of hydrogen.

We reported that Ni/Mg(Al)O catalyst derived from hydrotalcite(HT)-like compounds produced highly dispersed and stable Ni metal particles on the surfaces [4-9] and were successfully applied for the oxidative and steam reforming of CH_4 [6,7].

However, the Ni/Mg(Al)O catalysts were quickly deactivated due to the oxidation of Ni metal not only by oxygen but also by steam as the purge gas when they were applied in the daily start-up and shut-down (DSS) operation of steam reforming of CH_4 [10]. The loading of small amounts of noble metals on Ni/Mg(Al)O catalysts has been found to be effective for suppressing the Ni oxidation during the DSS operation [11-13].

In contrast to CH_4, only introductory studies have been published on noble metal catalysts concerning the partial oxidation of higher hydrocarbons [14-18]. The extensive work by Schmidt and co-workers on short contact-time reactors [14,15] showed that Rh has high activity and selectivity, superior to that of other noble metals. Rh-impregnated alumina foams and metallic microchannel reactors were studied for production of hydrogen-rich syngas through short contact-time catalytic partial oxidation of propane [17,18]. However, these noble metal-loaded catalysts do not seem acceptable for this process due to their high cost.

Only a few papers have reported on nickel-loaded catalysts for the partial oxidation of higher hydrocarbons [19,20] even including dry reforming [21]. Nickel supported catalysts were modified by alkali metal or rare-earth metal oxides [19]. Ni/Mg(Al)O catalysts were prepared from Mg-Al HT containing Ni at the Mg sites as the precursors [20,21]. As a bimetallic catalyst, Ni-Pt catalysts supported on δ-Al_2O_3 were successfully employed in both oxidative steam reformings and partial oxidations of propane and butane [22-24]. The superior catalytic performances of the bimetallic systems are due to the actions as micro heat exchangers; the heat generated by Pt sites during the exothermic total oxidation can readily be transferred through the catalyst

particles acting as micro heat exchangers to the Ni sites, which promote endothermic steam reforming.

Further extensive studies are indispensable for developing inexpensive and sustainable catalysts for the production of hydrogen as a future clean fuel. Recently we have reported that the loading of small amount of noble metals, i.e., Ru, Rh, Pd, Ir and Pt, on the Ni/Mg(Al)O catalysts effectively suppresses both coke formation and Ni oxidation in the partial oxidation of propane [25]. Among the noble metals tested, Ru seems to be the most promising judging from the loading effect [25]. In this contribution, we report some details of the improved behavior, i.e., self activation and the prominent effect of the reduction-oxidation treatment, of Ru-$Ni_{0.5}$/$Mg_{2.5}$(Al)O bimetallic catalysts in the partial oxidation of propane.

2. Experimental

2.1. Catalyst preparation

Ni-loaded Mg(Al)O catalyst with the Mg/Ni/Al composition of 2.5/0.5/1 was prepared by co-precipitation following the procedure shown in the previous work [25]; $Mg_{2.5}$($Ni_{0.5}$)-Al HT-like precursor was prepared by co-precipitation of the nitrates of the metal components and calcined in a muffle furnace to form $Mg_{2.5}$(Al,$Ni_{0.5}$)O periclase as the precursor of $Ni_{0.5}$/$Mg_{2.5}$(Al)O catalysts. Ni loading was 13.5 wt% by ICP analyses after the calcinination at 900 ºC. Mg_3(Al)O periclase was prepared from Mg_3-Al HT and calcined in a similar manner to the method above mentioned.

Loading of Ru has been performed by adopting a "memory effect" of Mg-Al HT [25,26]; 1.0 g of the powders of $Mg_{2.5}(Al,Ni_{0.5})O$ periclase were dipped in 5 ml of aqueous solution of appropriate amount of Ru(III) nitrate for 1 h at room temperature, and dried in air at 75 ºC for 0.5 h followed by at 105 ºC for one night. During the dipping, Mg(Ni)-Al HT was reconstituted from Mg(Al,Ni)O periclase due to the "memory effect," where Ru(III) species was not chemically incorporated but physically absorbed in the HT layered structure [27]. The sample was calcined at 850 ºC for 5 h to form the precursor of $Ru\text{-}Ni_{0.5}/Mg_{2.5}(Al)O$ catalysts. The powder of the precursor was pressed into a disc, crushed, sieved to the particles of 0.36-0.60 mmΦ and used in the partial oxidation reaction as it is or after the reduction. 0.1 wt%$Ru/Mg_3(Al)O$ was prepared using $Mg_3(Al)O$ periclase as the catalyst support in a similar manner.

As a control, *iw*-13.5 wt% $Ni/\gamma\text{-}Al_2O_3$ catalyst was prepared by an incipient wetness method using $\gamma\text{-}Al_2O_3$ and an aqueous solution of Ni(II) nitrate. Commercial Ni and Ru catalysts were supplied from Süd-Chemie Catalysts Japan, Inc. and were also used as controls. FCR (12 wt%$Ni/\alpha\text{-}Al_2O_3$) and RUA (2 wt%$Ru/\alpha\text{-}Al_2O_3$) as received were first crushed to fine powders, pressed into discs and roughly crushed; the particles of 0.36-0.60 mmΦ were used in the reforming reactions. BET surface area was 7.0 for FCR and 6.5 $m^2\ g_{cat}^{-1}$ for RUA as the particles.

2.2. Characterization of catalyst

The structure of the catalysts was studied by using XRD, TPR, TPO, ICP, N_2 and H_2 adsorption method.

Powder X-ray diffraction was recorded on a Mac Science MX18XHF-SRA

powder diffraction-meter with mono-chromatized Cu *Kα* radiation (λ = 0.154 nm) at 40 kV and 200 mA. The diffraction pattern was identified by comparing with those included in the JCPDS (Joint Committee of Powder Diffraction Standards) data base.

Temperature-programmed reduction (TPR) of the catalyst was performed at a heating rate of 10 ºC min^{-1} using a H_2/Ar (5/95 ml min^{-1}) mixed gas as reducing gas after passing through a 13X molecular sieve trap to remove water. A U-shaped quartz tube reactor (6 mm i.d.) equipped with a TCD for monitoring the H_2 consumption was used. Prior to the TPR measurements, the sample was calcined at 300 ºC for 2 h in an O_2/Ar (10/40 ml min^{-1}) mixed gas.

Temperature programmed oxidation (TPO) experiment was performed on the catalyst after the reaction from room temperature to 900 ºC at a heating rate of 2.5 ºC min^{-1} in an O_2/N_2 (5/20 ml min^{-1}) mixed gas. The amount of coke formed on the catalyst was estimated from the amount of CO_2 formed during the TPO experiment.

Inductively coupled plasma spectroscopy (ICP) measurements were carried out using a Perkin-Elmer OPTIMA 3000 spectrometer. The content of each metal component was determined after the sample was completely dissolved using diluted hydrochloric acid and a small amount of hydrofluoric acid.

The N_2 adsorption (-196 ºC) study was used to examine BET surface area of the catalysts and the Mg(Al,Ni)O periclase. The BET surface measurements were carried out on a Shimadzu Micromeritics Flowsorb 2300, and all samples (ca. 100 mg) were pretreated in a N_2 (10 ml min^{-1}) gas at 300 ºC for 1 h before the measurements.

The H_2 adsorption was carried out by static equilibrium method at ambient temperature using the pulse method. A 50 mg portion of the catalyst was reduced in a

H_2/N_2 (5/10 ml min^{-1}) mixed gas at 900 ºC for 1 h and used for the measurement. After the sample was cooled to room temperature in Ar atmosphere, every 1.0 cc of a 4.9 % H_2/N_2 mixed gas was pulsed at regular intervals. During the pulse experiment, the amount of H_2 in the effluent was monitored with a TCD-gas chromatograph.

2.3. Kinetic measurements

Partial oxidation of propane was conducted using a fixed bed-flow reactor in a $C_3H_8/O_2/N_2$ (10/18.7/71.3 ml min^{-1}) mixed gas over 50 mg of the catalyst for testing the activity under two types of the reaction mode (Fig. 1). In the mode A, the partial oxidation reaction (P_{ox}) was started at 600 °C with the $C_3H_8/O_2/N_2$ (10/18.7/71.3 ml min^{-1}) mixed gas after pre-reducing the catalyst at 900 °C with a H_2/N_2 (5/10 ml min^{-1}) mixed gas, and purged two times with an O_2/N_2 (18.7/71.3 ml min^{-1}) mixed gas at 700 °C during the P_{ox}; the sustainability of the catalyst against the deactivation due to the Ni oxidation with O_2 was tested. In the previous paper [25], the sustainability against the Ni oxidation has been tested by decreasing the reaction temperature from 700 ºC to 400 ºC under the reaction atmospheres. In the present work, more severe conditions, i.e., at higher temperature and in O_2 gas atmosphere, have been selected for testing the sustainability against the Ni oxidation. In the mode B, the reaction temperature was stepwise increased from 400 °C to 800 °C with the fresh catalyst before pre-reduction treatment; behavior of self-activation of the catalysts by the auto-reduction was tested during the reaction. In the latter mode, the P_{ox} was carried out with a continuous flow of the $C_3H_8/O_2/N_2$ (10/18.7/71.3 ml min^{-1}) mixed gas. The catalyst was particles of 0.36-0.60 mmΦ dispersed in 100 mg of quartz sand. A

U-shaped quartz tube reactor (6 mm i.d.) was used, with the catalyst bed near the bottom. The thermocouple to control the reaction temperature was placed at the center of the catalyst bed. Product gases were analyzed by online TCD-gas chromatography. The conversions of both propane and oxygen and the selectivity to the products were calculated using N_2 as the internal standard and the following equations:

$$C_3H_8 \text{ Conv.} = [(C_3H_{8in} - C_3H_{8out}) / C_3H_{8in}] \times 100$$

$$O_2 \text{ Conv.} = [(O_{2in} - O_{2out}) / O_{2in}] \times 100$$

$$H_2 \text{ Sel.} = (H_{2out} / X) \times 100$$

$$CO \text{ Sel.} = (CO_{out} / Y) \times 100$$

$$CO_2 \text{ Sel.} = (CO_{2out} / Y) \times 100$$

$$CH_4 \text{ Sel.} = (CH_{4out} / Y) \times 100$$

$$C_2H_4 \text{ Sel.} = (C_2H_{4out} \times 2 / Y) \times 100$$

$$C_2H_6 \text{ Sel.} = (C_2H_{6out} \times 2 / Y) \times 100$$

$$C_3H_6 \text{ Sel.} = (C_3H_{6out} \times 3 / Y) \times 100$$

$$H_2O \text{ Sel.} = (H_2O_{out} / X) \times 100$$

where

$$X = H_{2out} + H_2O_{out} + (CH_{4out} + C_2H_{4out}) \times 2 + (C_2H_{6out} + C_3H_{6out}) \times 3$$

$$Y = CO_{out} + CO_{2out} + CH_{4out} + (C_2H_{4out} + C_2H_{6out}) \times 2 + C_3H_{6out} \times 3$$

3. Results and discussion

3.1. Propane oxidation over the Ru-Ni/Mg(Al)O catalysts.

Partial oxidation of propane over Ni catalysts proceeds *via* combustion (1),

$$C_3H_8 + 5O_2 \rightarrow 3CO_2 + 4H_2O \qquad \Delta H^0_{298} = -2{,}046 \text{ kJ mol}^{-1} \quad (1)$$

followed by steam and dry reforming reactions (2 and 3). Water-gas shift reaction (4),

$$C_3H_8 + 3H_2O \rightarrow 3CO + 7H_2 \qquad \Delta H^0_{298} = +497 \text{ kJ mol}^{-1} \quad (2)$$

$$C_3H_8 + 3CO_2 \rightarrow 6CO + 4H_2 \qquad \Delta H^0_{298} = +620 \text{ kJ mol}^{-1} \quad (3)$$

$$CO + H_2O \rightarrow CO_2 + H_2 \qquad \Delta H^0_{298} = -41 \text{ kJ mol}^{-1} \quad (4)$$

methanation (5), dehydrogenation of propane (6) and coke formation from propane (7)

$$CO + 3H_2 \rightarrow CH_4 + H_2O \qquad \Delta H^0_{298} = -205 \text{ kJ mol}^{-1} \quad (5)$$

$$C_3H_8 \rightarrow C_3H_6 + H_2 \qquad \Delta H^0_{298} = +124 \text{ kJ mol}^{-1} \quad (6)$$

$$C_3H_8 \rightarrow 3C + 4H_2 \qquad \Delta H^0_{298} = +104 \text{ kJ mol}^{-1} \quad (7)$$

will play a role, depending on reactant composition, temperature and heat transfer rate, residence time and the catalytic system involved. Additional side reactions, including cracking of propane (8) and Boudouard reaction (9) must be considered; the latter is

$$C_3H_8 \rightarrow C_2H_4 + CH_4 \qquad \Delta H^0_{298} = +89 \text{ kJ mol}^{-1} \quad (8)$$

$$2CO \rightarrow C_{(s)} + CO_2 \qquad \Delta H^0_{298} = -172 \text{ kJ mol}^{-1} \quad (9)$$

particularly unwanted and generally occurs when the O_2/C_3H_8 ratio in the reaction mixture becomes too low.

The Ru-Ni/Mg(Al)O catalysts have been prepared by dipping the powder of $Mg_{2.5}(Al,Ni_{0.5})O$ periclase in aqueous solutions of appropriate amounts of Ru(III) nitrate, as shown in Table 1 [25]; the 0.1 wt%Ru-$Ni_{0.5}/Mg_{2.5}(Al)O$ catalyst was prepared by dipping in 5 ml aqueous solution of Ru(III) nitrate for 1 h. During the dipping, the reconstitution of $Mg_{2.5}(Ni_{0.5})$-Al HT took place from $Mg_{2.5}(Al,Ni_{0.5})O$ periclase; Ni(II) species was still incorporated in the HT phase, whereas Ru(III) species was physically

adsorbed in the surface HT layer reconstituted since Ru(III) cannot be incorporated in the HT structure [27]. No reflection line was observed for any Ru species in the XRD patterns of the samples after the calcination followed by the reduction. Ru must be well dispersed on the reduced samples and well interacted with also finely dispersed Ni metal particles derived from the $Mg_{2.5}(Ni_{0.5})$-Al HT phase [4-9]. The interaction between Ni and Ru was estimated by the decrease in the reduction temperature of Ni in the TPR measurements (*vide infra*) [12,25]. Use of a small amount of the solution, i.e., 5 ml, sufficiently decreased the Ni reduction temperature from 887 °C for the $Ni_{0.5}/Mg_{2.5}(Al)O$ catalyst to 840 °C for the 0.1 wt%Ru-$Ni_{0.5}/Mg_{2.5}(Al)O$ catalyst [25].

According to the XRD analyses of the samples after the dipping and after the calcination, the 0.1 wt%Ru-$Ni_{0.5}/Mg_{2.5}(Al)O$ showed a weak reconstitution of HT. No distinct shift was observed in the reflection lines of the HT of all the samples prepared; this indicates that no substantial replacement of the Al^{3+} sites with Ru(III) ions took place and that Ru existed in the amorphous phase separately from the HT [27], judging from the larger size of the Ru^{3+} ions (0.068 nm) in comparison with the Al^{3+} ions (0.053 nm) [28].

The results of propane oxidation in the temperature-cycled mode between 400 °C and 700 °C showed that the 0.1 wt%Ru-$Ni_{0.5}/Mg_{2.5}(Al)O$ catalyst was the most active and sustainable among the catalysts tested [25]. In the previous paper [11,12], the Ru loading has been done by dipping 1.0 g of $Mg_{2.5}(Al,Ni_{0.5})O$ periclase powder in 40 ml of Ru(III) nitrate-solution for 12 h; the reconstitution of HT was almost completed. However, it was concluded that such intensive reconstitution of HT is not always necessary for the catalytic activity; only 5 ml of the Ru(III) nitrate-solution and 1 h of

the dipping time were enough for preparing the active catalyst as seen in the high dispersion for 0.1 wt%Ru-$Ni_{0.5}/Mg_{2.5}$(Al)O (Table 1) [25]. As reported in the previous paper [25], only surface reconstitution using 5 ml of the Ru(III) nitrate-solution and 1 h of the dipping time is enough for preparing the catalyst of good property. Moreover, water must be removed by the evaporation after the dipping treatment. When a large amount of the aqueous solution was used, an intensive reconstitution of the HT took place on the samples since the samples were necessarily dipped in the solution for a long term until the water was completely evaporated. Coking on the catalyst was also effectively reduced by this preparation method using 5 ml of the Ru(III) nitrate-solution and 1 h of the dipping time [25].

3.2. Sustainability of the Ru-Ni/Mg(Al)O catalysts.

The effects of Ru addition on the activity of the $Ni_{0.5}/Mg_{2.5}$(Al)O catalyst were studied in the partial oxidation of propane by the mode A (Fig. 1A) under the O_2 purging. The P_{ox} reaction at 600 °C for 1.5 h, interrupted by the O_2 purging at 700 °C for 1 h, was repeated three times after the reduction treatment of the catalysts with H_2/N_2 (5/10 ml min^{-1}) mixed gas at 900 °C for 30 min (Fig. 2). The results of propane oxidation over the 0.1 wt%Ru-$Ni_{0.5}/Mg_{2.5}$(Al)O catalyst (Fig. 2A) are compared with those over the $Ni_{0.5}/Mg_{2.5}$(Al)O catalyst (Fig. 2B). After the reduction pre-treatment, both catalysts showed high activity for the syngas production, although the former Ni-Ru bimetallic catalyst showed higher propane conversion than the latter Ni catalyst.

The $Ni_{0.5}/Mg_{2.5}$(Al)O catalyst showed a significant deactivation after the 1^{st} O_2 purging (Fig. 2B), certainly due to the oxidation of Ni metal to Ni^{2+} which was probably

incorporated into the lattice of $Mg_{2.5}(Al,Ni_{0.5})O$ periclase [10]. After the deactivation, the selectivity to both CO_2 and H_2O increased at the 2nd operation, while that rather decreased at the 3rd operation. Instead, the selectivity to both C_3H_6 and C_2H_4 increased after repeating the O_2 purging, suggesting that oxidative dehydrogenation and thermal cracking were accelerated after the O_2 purging. The activity of the $Ni_{0.5}/Mg_{2.5}(Al)O$ catalyst was almost recovered by the H_2 reduction treatment at 900 °C, but the catalyst was deactivated again by repeating the O_2 purging.

On the other hand, the 0.1 wt%Ru-$Ni_{0.5}/Mg_{2.5}(Al)O$ catalyst survived and produced syngas even after the repeated O_2 purging, although the propane conversion was slightly decreased together with the selectivity to CH_4 (Fig. 2A). It is interesting to note that the selectivity to both H_2 and CO gradually increased by repeating the O_2 purging. After the H_2 reduction treatment, the activity of the 0.1 wt%Ru-$Ni_{0.5}/Mg_{2.5}(Al)O$ catalyst shown by propane conversion was perfectly recovered. This catalyst showed high activity for the syngas formation throughout the reaction. Judging from the product distributions during the reaction, we conclude that the 0.1 wt%Ru-$Ni_{0.5}/Mg_{2.5}(Al)O$ catalyst was sustainable and effectively promoted the syngas formation reactions by the following mechanism: propane combustion (1), followed by reforming reactions (2) and (3), coupled with water-gas shift reaction (4) and methanation (5).

3.3. Self-activation of the Ru-Ni/Mg(Al)O catalysts.

Propane oxidation was carried out by the mode B (Fig. 1B) over the Ru-Ni/Mg(Al)O catalysts, i.e., by stepwise increasing the temperature from 400 °C to

800 °C; the conversion of propane and the rate of H_2 production during the reaction are shown in Fig. 3. The reaction was carried out over the catalyst before the H_2 reduction pre-treatment. Over all catalysts tested, propane conversion was less than 15 % below 600 °C, although it gradually increased with increasing the reaction temperature. Above 700 °C, propane was almost completely consumed and no significant effect of the Ru loading on the propane conversion was observed. However, the rate of H_2 production was below 2 mol $h^{-1}g_{cat}^{-1}$ on the $Ni_{0.5}/Mg_{2.5}(Al)O$ catalysts with the Ru loading below 0.05 wt%, while the rate was clearly enhanced by the Ru loading above 0.1 wt%. It must be noted that both $Ni_{0.5}/Mg_{2.5}(Al)O$ and 0.01 wt%Ru-$Ni_{0.5}/Mg_{2.5}(Al)O$ catalysts showed extremely low rates of H_2 production (~ 0.5 mol h^{-1} g_{cat}^{-1}) even at 800 °C although propane conversion was high around 100 %.

The product distributions in the propane oxidation over the $Mg_{2.5}(Al,Ni_{0.5})O$ and 0.1 wt%Ru-$Mg_{2.5}(Al,Ni_{0.5})O$ precursor are shown in Figs. 4A and B, respectively. The former showed low selectivity to CO and H_2 even above 700 °C although high propane conversion was attained (Fig. 4B). The selectivity to H_2 was extremely low, whereas the selectivities to C_2H_4, H_2O and CH_4 were rather high. Below 600 °C, the formations of C_2 and C_3 compounds were observed together with CO. The selectivity to CO_2 was not comparable to that of H_2O. All these results indicate that the $Mg_{2.5}(Al,Ni_{0.5})O$ precursor substantially promoted the thermal cracking together with the combustion reaction. The color was still green in an inlet part of the catalyst bed, while it changed to grey only in a small part of the outlet, indicating that Ni was not reduced and existed mainly in the valence state of Ni^{2+}. The reaction of propane on the $Mg_{2.5}(Al,Ni_{0.5})O$ precursor seems to be complex and cannot be explained by a simple mechanism. This is probably due to

the fact that the valence state of the surface Ni species on the catalyst changed depending on the atmosphere in the reaction gases.

On the other hand, the behavior of the 0.1 wt%Ru-$Mg_{2.5}(Al,Ni_{0.5})O$ precursor in the partial oxidation of propane is well explained by the mechanism of combustion at low temperature followed by reforming at increasing temperature (Fig. 4A). Below 500 °C, the 0.1 wt%Ru-$Mg_{2.5}(Al,Ni_{0.5})O$ catalyzed the propane combustion to form mainly CO_2 and H_2O with both high selectivities, suggesting that Ru assisted the propane combustion on the Ni^{2+} sites. Judging from the molar ratio of $C_3H_8/O_2 = 2/3$ and the reaction stoichiometry of combustion (1), propane conversion is calculated as 30 % when propane combustion alone proceeds. Actually propane conversion was always lower than 30 % below 600 °C, indicating that only a part of propane was consumed by the combustion reactions. When the reaction temperature was increased above 700 °C, propane conversion suddenly increased. Simultaneously the selectivities to both CO_2 and H_2O decreased, whereas those to CO and H_2 increased, indicating that the reforming reactions (2 and 3) began to follow the combustion reaction (1). The color of the catalyst changed to grey throughout the catalyst bed after the reaction, indicating that all Ni species was reduced to the metallic state. Actually the reflections of Ni metal were observed in the XRD patterns of the Ru-Ni catalyst after the reaction. These clearly indicate that 0.1 wt%Ru-$Mg_{2.5}(Al,Ni_{0.5})O$ was self-activated to the reduced form, i.e., 0.1 wt%Ru-$Ni_{0.5-x}/Mg_{2.5}(Al,Ni_x)O$ (the reduction degree of $Mg_{2.5}(Al,Ni_{0.5})O$ was around 85 % [12]), during the reaction and catalyzed the partial oxidation of propane to syngas. It is likely that Ru assists the self-reduction of Ni under the reaction atmosphere due to the spillover of hydrogen from Ru to Ni (*vide infra*).

3.4. Sustainability of the Ru-Ni/Mg(Al)O catalysts against the O_2 purge.

Several Ni, Ru or Ni-Ru bimetal loaded catalysts including commercial one have been tested in the partial oxidation of propane at 600 °C under the O_2 purge by the reaction mode A (Fig. 1A); propane conversion and H_2 selectivity during the reaction are shown in Fig. 5. Commercial Ru catalyst (RUA) showed sustainability against the O_2 purge although the activity was not high enough; both propane conversion and H_2 selectivity gradually decreased during stepwise O_2 purging (Fig. 5A). On the other hand, supported Ni catalysts, i.e., $Ni_{0.5}/Mg_{2.5}(Al)O$ and *iw*-13.5 wt%Ni/γ-Al_2O_3, showed a significant deactivation after the 1st O_2 purge; the selectivity to H_2 decreased over all the Ni catalysts. Commercial Ni catalyst (FCR) showed no significant decrease in the propane conversion but kept the low selectivity to H_2 throughout the reaction. The 0.1 wt%$Ru/Mg_3(Al)O$ catalyst showed low but stable values in both propane conversion and H_2 selectivity during the reaction, indicating that the amount of Ru loading was not sufficient to reveal the activity (Fig. 5A).

On $Ni_{0.5}/Mg_{2.5}(Al)O$, the Ru loading above 0.05 wt% gave rise to no deactivation even after the repeated O_2 purging, while the 0.01 wt% Ru loading resulted in a significant deactivation just after the 1st O_2 purge (Fig. 5B). After the reaction, the color of all Ni catalysts deactivated was green, while those of 0.05-0.5 wt%Ru-loaded $Ni_{0.5}/Mg_{2.5}(Al)O$ catalysts kept the grey color observed just after the reduction pre-treatment. It seems that the Ru loading above 0.05 wt% was effective to keep the Ni species in the active reduced form on the $Ni_{0.5}/Mg_{2.5}(Al)O$ catalyst. The highest values in both selectivity and rate of H_2 formation were obtained with 0.1 wt% Ru loading,

although propane conversion decreased during the reaction. It must be noted that the selectivity to H_2 stepwise increased after each O_2 purging for 0.05-0.5 wt%Ru-loaded $Ni_{0.5}/Mg_{2.5}(Al)O$ catalysts (Fig. 5B). This will be later discussed in connection with the activity for self-activation of the Ru-Ni/Mg(Al)O catalysts (*vide infra*).

3.5. Effect of the H_2/O_2 treatment on the activity of the Ru-Ni/Mg(Al)O catalysts.

As mentioned previously, the activity of the 0.05-0.5 wt%Ru-$Ni_{0.5}/Mg_{2.5}(Al)O$ catalysts for propane reforming increased by the O_2 treatment (Figs. 2A and 5B). The effect of O_2 treatment on the reforming activity was further investigated by the H_2 reduction followed by the O_2 oxidation treatment (H_2/O_2 treatment) of the Ru-$Ni_{0.5}/Mg_{2.5}(Al)O$ catalysts under increasing temperature (Fig. 6). The catalysts were first tested in the propane oxidation without H_2 reduction pre-treatment and then tested again in the propane oxidation after the H_2/O_2 treatment, i.e., after the reduction with H_2/N_2 (5/10 ml min^{-1}) at 900 ºC for 1 h followed by the oxidation with O_2/N_2 (19/71 ml min^{-1}) at 700 ºC for 1 h. After the H_2/O_2 treatment, the propane conversion increased clearly at the reaction temperature below 600 °C (Fig. 6). The propane conversions at 600 °C before and after the H_2/O_2 treatment were each plotted against the Ru loading (Fig. 6B); no significant change by the Ru loading was observed in the propane conversion on the catalysts before the H_2/O_2 treatment, whereas the propane conversion increased with the Ru loading after the H_2/O_2 treatment. These results suggest that the surface state of Ni-Ru bimetallic system substantially changed during the H_2/O_2 treatment. Actually the propane conversion increased with increasing Ru loading after

the H_2/O_2 treatment, indicating that the treatment strongly affects the surface state of Ni species on the Ru-Ni bimetallic catalysts.

XRD patterns of the $Ni_{0.5}/Mg_{2.5}(Al)O$, 0.05 wt%Ru-$Ni_{0.5}/Mg_{2.5}(Al)O$ and 0.1 wt%Ru-$Ni_{0.5}/Mg_{2.5}(Al)O$ catalysts during the H_2/O_2 treatment are shown in Figs. 7 A, B and C, respectively. All catalysts before reduction showed only reflection lines of $Mg_{2.5}(Al,Ni_{0.5})O$ periclase (Fig. 7Aa, Ba and Ca). After the reduction with H_2, the reflection lines of the periclase were weakened and replaced by those of Ni metal; the latter reflections were observed more sharply for the $Ni_{0.5}/Mg_{2.5}(Al)O$ catalyst (Fig. 7Ab) than for the 0.1 wt%Ru-$Ni_{0.5}/Mg_{2.5}(Al)O$ catalyst (Fig. 7Cb). After the H_2/O_2 treatment, the reflection intensity of the periclase was re-enhanced, while that of Ni metal was weakened more significantly for the $Ni_{0.5}/Mg_{2.5}(Al)O$ catalyst (Fig. 7Ac) than for the 0.1 wt%Ru-$Ni_{0.5}/Mg_{2.5}(Al)O$ catalyst (Fig. 7Cc). When these catalysts were tested in the propane oxidation by increasing temperature by the mode B (Fig. 1B), weak and broad lines of Ni metal were observed for all catalysts; the intensity became stronger with increasing the Ru loading (Fig. 7Ad - Cd). It is interesting to note that the lines of Ni metal were always broad and remained even after the O_2 treatment on the 0.1 wt%Ru-$Ni_{0.5}/Mg_{2.5}(Al)O$ catalyst during the H_2/O_2 treatment followed by the reaction, although the line intensities changed depending on the treatment stages. These results suggest that Ni metal particles became finely dispersed and stable on the 0.1 wt%Ru-$Ni_{0.5}/Mg_{2.5}(Al)O$ catalyst during the H_2/O_2 treatment. It is most likely that such Ni metal species coupled with Ru enhanced the catalytic activity at 600 °C by the self-activation mechanism.

3.6. Active species on the Ru-Ni/Mg(Al)O catalysts after the H_2/O_2 treatment.

The results of TPR measurements of the Ru-Ni/Mg(Al)O catalysts after the H_2/O_2 treatment together with the fresh catalyst are shown in Fig. 8. Asreported in the previous paper [25], the reduction peak of Ni appeared at 887 °C for the fresh $Ni_{0.5}/Mg_{2.5}(Al)O$ catalyst; the reduction temperature decreased with increasing the Ru loading and finally reached 820 °C for the 0.5 wt%Ru-$Ni_{0.5}/Mg_{2.5}(Al)O$ catalyst. The peak observed at 887 °C can be assigned to the Ni^{2+} ions located deep in the MgO lattice due to the formation of Mg(Al,Ni)O periclase as solid solutions [29,30]. The NiO-MgO solid solutions alone prepared by the calcination at the temperature above 850 °C showed no reduction peak up to 1100 °C [5]. Due to the replacement of the Mg^{2+} sites by Al^{3+} ions in the NiO-MgO solid solutions, the lattice defects were produced in the Mg(Al,Ni)O periclase, resulting in a decrease of the Ni reduction temperature. Moreover, the co-presence of Ru caused a further decrease in the reduction temperature of Ni in the Mg(Al,Ni)O periclase due to its easy reduction by H_2 dissociation, followed by the spillover of hydrogen to Ni. The weak and broad peak observed around 400 ºC for 0.5 wt%Ru-$Ni_{0.5}/Mg_{2.5}(Al)O$ catalyst (Fig. 8e) can be ascribed to the reduction of RuO_2 to Ru metal, since no other stable ruthenium oxides are known to exist in the solid state [31,32]. This indicates that a part of Ru was separated from Ni-Ru binary system on the 0.5 wt%Ru-$Ni_{0.5}/Mg_{2.5}(Al)O$ catalyst.

After the H_2/O_2 treatment, the reduction peak of Ni observed between 800 and 900 °C shifted toward the lower temperature and was separated into two peaks, i.e., around 550 °C and 750 °C. H_2 consumption of each of the two peaks was estimated by the peak deconvolution, and values are shown in Fig. 9 together with those of H_2

consumption of the fresh samples. Summation of the two H_2 consumptions after the H_2/O_2 treatment well coincides with that of fresh sample, suggesting that H_2 was mainly consumed on the Ni metal species on the catalysts. This observation is reasonable considering that the amount of Ru loaded is remarkably small compared to that of Ni. The 1st H_2 consumption observed at 550 °C decreased with increasing the Ru loading, whereas the 2nd H_2 consumption observed at 750 °C increased with increasing the Ru loading (Fig. 9). It was reported that the peak at 530 °C in the TPR of Ni/MgO catalysts can be assigned to Ni^{2+} ions having square-pyramidal coordination in the outermost layer of the MgO structure [29]. Pure NiO has a reduction peak around 385 °C [5], while Ni/γ-Al_2O_3 catalyst has a peak at 410 °C assigned to the reduction of separated NiO [33]. It was reported that the Ni/γ-Al_2O_3 sample prepared by impregnation showed two peaks in the TPR ascribed to the reduction of the two differently coordinated surface-dispersed nickel oxide species, i.e., octahedral (527 °C) and tetrahedral (687 °C) site nickel [34]. However, the latter peak was not observed in the present sample (Fig. 8). Therefore, it is likely that Ni species detected by the 1st peak are composed of Ni^{2+} ions having square-pyramidal coordination in the outermost layer of the Mg(Al)O structure and are probably produced during the oxidation treatment. These species probably show no significant contribution on the catalytic activity since the H_2 consumption decreased with increasing Ru loading (Fig. 9). On the other hand, Ni species observed by the 2nd peak at 750 °C revealed increasing H_2 consumption with increasing Ru loading, being relatively well correlated with the relationship between catalytic activity and Ru loading shown in Fig. 6B. It is likely that Ni species on the Ru-Ni/Mg(Al)O catalysts after the H_2/O_2 treatment can be classified into two types; the

1st consumed H_2 at 550 °C and showed no affirmative effect on the catalytic activity, whereas the 2nd consumed H_2 at 750 °C and contributed to the activity for the propane oxidation.

It is supposed that Ni species are reduced and liberated from Mg(Al,Ni)O periclase structure during the H_2 treatment and finally appeared as Ni metal particles on the surface of the periclase particles. Such reduced Ni species must be finely dispersed and also keep a good contact with Ru species on the Mg(Al)O periclase, since Ru was also finely dispersed in the HT layer reconstituted on the surface of the Mg(Al)O periclase. After the H_2/O_2 treatment, the Ni species are oxidized to form two types of Ni species on the catalyst surface: i.e., the 1st is composed of Ni^{2+} ions having square-pyramidal coordination in the outermost layer of the MgO structure, whereas the 2nd is probably composed of Ni species in the Ni-Ru bimetallic complexes formed on the Mg(Al)O periclase. The 1st is not sufficiently active after the reduction with H_2, while the 2nd is converted to finely dispersed Ni metal particles which show high activity being assisted by Ru. Increase in the activity with increasing Ru content at 600 °C observed in Fig. 6B is certainly due to the self-activation of Ni-Ru catalysts, which is certainly provoked by spillover of hydrogen from Ru to Ni. The higher dispersions of Ni and Ru metal particles as well as a good contact between them are preferable for the effective spillover of hydrogen. It is most likely that, during the H_2/O_2 pre-treatment, both Ni and Ru metals were finely dispersed and well contacted each other, resulting in the high catalytic activity.

5. Conclusion

0.1~0.5 wt%Ru-$Ni_{0.5}/Mg_{2.5}$(Al)O catalysts have been prepared by dipping $Mg_{2.5}(Al,Ni_{0.5})O$ periclase in an aqueous solution of Ru(III) nitrate. The reconstitution of Mg(Ni)-Al HT took place on the surface of the $Mg_{2.5}(Al,Ni_{0.5})O$ periclase *via* the "memory effect" of hydrotalcite, where Ru(III) ions are trapped in the HT layered structure, resulting in the highly dispersed Ni-Ru bimetallic system after the reduction. Only 0.1 wt% of the Ru loading afforded the high activity as well as the high sustainability on $Ni_{0.5}/Mg_{2.5}$(Al)O catalyst in the O_2 purged propane partial oxidation. By the reduction followed by the oxidation treatment of the Ru-Ni/Mg(Al)O catalysts, Ni metal species were transformed into two types of species: one is composed of Ni^{2+} ions having square-pyramidal coordination in the outermost layer of the MgO structure, and the other forms Ni-Ru bimetallic complexes on the surface of the $Mg_{2.5}(Al,Ni_{0.5})O$ periclase. The latter is converted to finely dispersed Ni metal particles that show high activity, assisted by Ru in the partial oxidation of propane. The self-activation of Ru-Ni/Mg(Al)O catalysts was observed due to the Ni reduction provoked by spillover of hydrogen from Ru to Ni during the reaction.

References

1 M.A. Peña, J.P. Gómez, J.L.G. Fierro, Appl. Catal. A 144 (1996) 7.

2 J.N. Armor, Appl. Catal. A 176 (1999) 159.

3 J.R. Rostrup-Nielsen, Catal. Today 71 (2002) 243.

4 T. Shishido, M. Sukenobu, H. Morioka, R. Furukawa, H. Shirahase, K. Takehira, Catal. Lett. 73 (2001) 21.

5 T. Shishido, M. Sukenobu, H. Morioka, M. Kondo, Y. Wang, K. Takaki, K. Takehira, Appl. Catal. A 223 (2002) 35.

6 K. Takehira, T. Shishido, P. Wang, T. Kosaka, K. Takaki, Phys. Chem. Chem. Phys. 5 (2003) 3801.

7 K. Takehira, T. Shishido, P. Wang, T. Kosaka, K. Takaki, J. Catal. 221 (2004) 43.

8 K. Takehira, T. Shishido, D. Shouro, K. Murakami, M. Honda, T. Kawabata, K. Takaki, Appl. Catal. A 279 (2005) 41.

9 K. Takehira, T. Kawabata, T. Shishido, K. Murakami, T. Ohi, D. Shoro, M. Honda, K. Takaki, J. Catal. 231 (2005) 92.

10 T. Ohi, T. Miyata, D. Li, T. Shishido, T. Kawabata, T. Sano, K. Takehira, Appl. Catal. A 308 (2006) 194.

11 T. Miyata, D. Li, M. Shiraga, T. Shishido, Y. Oumi, T. Sano, K. Takehira, Appl. Catal. A 310 (2006) 97.

12 T. Miyata, M. Shiraga, D. Li, I. Atake, T. Shishido, Y. Oumi, T. Sano, K. Takehira, Catal. Commun. 8 (2007) 447.

13 A.I. Tsyganok, M. Inaba, T. Tsunoda, K. Uchida, K. Suzuki, K. Takehira, T. Hayakawa, Appl. Catal. A 292 (2005) 328.

14 D.A. Goetsch, L.D. Schmidt, Science 271 (1996) 1560.

15 A.S. Bodke, S.S. Bharadwaj, L.D. Schmidt, J. Catal. 179 (1998) 138.

16 S. Ayabe, H. Omoto, T. Utaka, R. Kikuchi, K. Sasaki, Y. Teraoka, K. Eguchi, Appl. Catal. A 241 (2003) 261.

17 I. Aartun, T. Gjervan, H. Venvik, O. Görke, P. Pfeifer, M. Fathi, A. Holmen, K. Schubert, Chem. Eng. J. 101 (2004) 93.

18 B. Silberova, H.J. Venvik, A. Holmen, Catal. Today 99 (2005) 69.

19 S. Liu, L. Xu, S. Xie, Q. Wang, G. Xiong, Appl. Catal. A 211 (2001) 145.

20 K. Schulze, W. Makowski, R. Chyży, R. Dziembaj, G. Geismar, Appl. Clay Sci. 18 (2001) 59.

21 A. Olafsen, Å. Slagtern, I.M. Dahl, U. Olsbye, Y. Schuurman, C. Mirodatos, J. Catal. 229 (2005) 163.

22 A.K. Avci, D.L. Trimm, A.E. Aksoylu, Z.İ. Önsan, Catal. Lett. 88 (2003) 17.

23 A.K. Avci, D.L. Trimm, A.E. Aksoylu, Z.İ. Önsan, Appl. Catal. A 258 (2004) 235.

24 B.S. Çağlayan, A.K. Avci, Z.İ. Önsan, A.E. Aksoylu, Appl. Catal. A 280 (2005) 181.

25 M. Shiraga, D. Li, I. Atake, T. Shishido, Y. Oumi, T. Sano, K. Takehira, Appl. Catal. A 318 (2007) 143.

26 F. Cavani, F. Trifirò, A. Vaccari, Catal. Today 11 (1991) 173.

27 F. Basile, G. Fornasari, M. Gazzano, A. Vaccari, Appl. Clay Sci. 16 (2000) 185.

28 R.D. Shannon, Acta Crystallogr. A 32 (1976) 751.

29 S. Freni, S. Cavallaro, N. Mondello, L. Spadaro, F. Frusteri, Catal. Commun. 4 (2003) 259.

30 T. Furusawa, A. Tsutsumi, Appl. Catal. A 278 (2005) 207.

31 H. Madhavaram, H. Idriss, S. Wendt, Y.D. Kim, M. Knapp, H. Over, J. Aβmann, E. Löffler, M. Muhler, J. Catal. 202 (2001) 296.

32 I. Balint, A. Miyazaki, K. Aika, J. Catal. 220 (2003) 74.

33 G. Li, L. Hu, J.M. Hill, Appl. Catal. A 301 (2006) 16.

34 J. Wang, L. Dong, Y. Hu, G. Zheng, Z. Hu, Y. Chen, J. Solid State Chem. 157 (2001) 274.

Table 1. Physicochemical properties of Ru-$Ni_{0.5}/Mg_{2.5}(Al)O$ catalysts [25]

Catalyst[a]	BET surface area[b] / $m^2\ g_{cat}^{-1}$	H_2 uptake[c] / $\mu mol\ g_{cat}^{-1}$	Dispersion[d] / %	Particle size of Ni metal / nm	
				XRD[e]	H_2 up take[d]
$Ni_{0.5}/Mg_{2.5}(Al)O$	158.0	120.7	13.1	6.9	7.4
iw-13.5wt%Ni/γ-Al_2O_3	106.3	74.4	6.5	10.0	14.9[f]
0.1wt%Ru/$Mg_3(Al)O$	121.5	0.56	-	-	-
0.5wt%Ru-$Ni_{0.5}/Mg_{2.5}(Al)O$	148.0	261.4	28.3	5.0	3.4
0.1wt%Ru-$Ni_{0.5}/Mg_{2.5}(Al)O$	146.7	221.9	24.0	5.2	4.0
0.05wt%Ru-$Ni_{0.5}/Mg_{2.5}(Al)O$	138.3	187.2	20.3	5.7	4.8
0.01wt%Ru-$Ni_{0.5}/Mg_{2.5}(Al)O$	137.7	183.5	19.9	5.7	4.9
FCR	7.0	-	-	-	-
RUA	6.5	-	-	-	-

a) Metal loading was carried out by dipping 1.0 g of the powder of $Ni_{0.5}/Mg_{2.5}(Al)O$ in 5 ml of aqueous solution of the nitrates of noble metals for 1 h at room temperature.

b) Calcined at 850 ºC for 5 h.

c) Determined by the H_2 pulse method.

d) Calculated from the H_2 uptake assuming the reduction degree of 80 % for hydrotalcite derived catalyst [12] and 100 % for impregnated catalyst. [f]

e) Calculated from the full width at half maximum of the reflection of Ni (200) plane in the XRD using the Scherrer equation.

Figure captions

Fig. 1 Reaction modes for the partial oxidation of propane.

A: by O_2 purging; B: by increasing reaction temperature.

Fig. 2 Partial oxidation of propane over the 0.1 wt%Ru-$Ni_{0.5}/Mg_{2.5}$(Al)O (A) and $Ni_{0.5}/Mg_{2.5}$(Al)O (B) catalysts under O_2 purging.

Catalyst, 50 mg with quartz sand 100 mg; reaction temperature, 600 °C; $C_3H_8/O_2/N_2$ = 10/18.7/71.3 ml min^{-1}; GHSV = 120,000 ml h^{-1} g_{cat}^{-1}.

Conversion: ×, propane; selectivity: ●, H_2; ■, CO; ▲, CO_2; ✻, H_2O; ○, CH_4; □, C_2H_4; Δ, C_2H_6; +, C_3H_6.

O_2 purge, by O_2/N_2 (18.7/71.3 ml min^{-1}) at 700 °C each 1.5 h of the reaction time; reduction treatment, by H_2/N_2 (5/10 ml min^{-1}) at 900 °C at 4.5 h of the reaction time.

Fig. 3 Partial oxidation of propane over the Ru-$Ni_{0.5}/Mg_{2.5}$(Al)O catalysts under increasing temperature.

Catalyst, 50 mg with quartz sand 200 mg; $C_3H_8/O_2/N_2$ = 10/18.7/71.3 ml min^{-1}; GHSV = 120,000 ml h^{-1} g_{cat}^{-1}.

●, $Ni_{0.5}/Mg_{2.5}$(Al)O; ■, 0.5 wt%Ru-$Ni_{0.5}/Mg_{2.5}$(Al)O; ▲, 0.1 wt%Ru-$Ni_{0.5}/Mg_{2.5}$(Al)O; ○, 0.05 wt%Ru-$Ni_{0.5}/Mg_{2.5}$(Al)O; □, 0.01 wt%Ru-$Ni_{0.5}/Mg_{2.5}$(Al)O; Δ, 0.1 wt%Ru/Mg_3(Al)O.

Full line, propane conversion; dotted line, rate of H_2 production.

Fig. 4 Partial oxidation of propane over the 0.1 wt%Ru-$Ni_{0.5}/Mg_{2.5}$(Al)O (A) and $Ni_{0.5}/Mg_{2.5}$(Al)O (B) catalysts under increasing temperature.

Catalyst, 50 mg with quartz sand 100 mg; $C_3H_8/O_2/N_2$ = 10/18.7/71.3 ml min^{-1}; GHSV = 120,000 ml h^{-1} g_{cat}^{-1}.

Conversion: ×, propane; selectivity: ●, H_2; ■, CO; ▲, CO_2; ✻, H_2O; ○, CH_4; □, C_2H_4; Δ, C_2H_6; +, C_3H_6.

Full line, left hand side scale; dotted line, right hand side scale.

Fig. 5 Effect of O_2 purge on the partial oxidation of propane.

Catalyst, 50 mg with quartz sand 100 mg; reaction temperature, 700 °C; $C_3H_8/O_2/N_2$ = 10/18.7/71.3 ml min^{-1}; GHSV = 120,000 ml h^{-1} g_{cat}^{-1}; O_2 purge, O_2/N_2 (18.7/71.3 ml min^{-1})

A: ●, $Ni_{0.5}/Mg_{2.5}(Al)O$; ■, FCR; ▲, RUA; ○, *iw*-13.5 wt%Ni/γ-Al_2O_3; ; □, 0.1 wt%Ru/$Mg_3(Al)O$.

B: ●, 0.5 wt%Ru-$Ni_{0.5}/Mg_{2.5}(Al)O$; ■, 0.1 wt%Ru-$Ni_{0.5}/Mg_{2.5}(Al)O$; ▲, 0.05 wt%Ru-$Ni_{0.5}/Mg_{2.5}(Al)O$; ○, 0.01 wt%Ru-$Ni_{0.5}/Mg_{2.5}(Al)O$.

Full line, propane conversion; dotted line, H_2, selectivity.

Fig. 6 Effect of oxidation treatment on the activity of the Ru-$Ni_{0.5}Mg_{2.5}(Al)O$ catalysts.

Catalyst, 50 mg with quartz sand 100 mg; $C_3H_8/O_2/N_2$ = 10/18.7/71.3 ml min^{-1}; GHSV = 120,000 ml h^{-1} g_{cat}^{-1}.

A: Time course of the reaction under increasing temperature; ●, $Ni_{0.5}/Mg_{2.5}(Al)O$; ■, 0.5 wt%Ru-$Ni_{0.5}/Mg_{2.5}(Al)O$; ▲, 0.1 wt%Ru-$Ni_{0.5}/Mg_{2.5}(Al)O$; ○, 0.05 wt%Ru-$Ni_{0.5}/Mg_{2.5}(Al)O$.

Full line, fresh catalysts; dotted line, catalysts after the reduction with H_2/N_2 (5/10 ml min^{-1}) at 900 ºC for 1 h, followed by the oxidation with O_2/N_2

(18.7/71.3 ml min^{-1}) at 700 ºC for 1 h.

B: Propane conversion at 600 °C; ●, fresh catalysts; ■, catalysts after the reduction with H_2/N_2 (5/10 ml min^{-1}) at 900 ºC for 1 h, followed by the oxidation with O_2/N_2 (18.7/71.3 ml min^{-1}) at 700 ºC for 1 h.

Fig. 7 XRD patterns of the $Ni_{0.5}/Mg_{2.5}(Al)O$ (A), 0.05 wt%Ru-$Ni_{0.5}/Mg_{2.5}(Al)O$ (B) and 0.1 wt%Ru-$Ni_{0.5}/Mg_{2.5}(Al)O$ (C) catalysts at different stages.

a) before H_2 reduction; b) after H_2 reduction; c) after O_2 treatment; d) after reaction.

○, Mg(Al,Ni)O periclase; ●, Ni metal.

Fig. 8 Temperature programmed reduction of supported Ru-Ni catalysts.

a) $Ni_{0.5}/Mg_{2.5}(Al)O$; b) 0.01 wt%Ru-$Ni_{0.5}/Mg_{2.5}(Al)O$; c) 0.05 wt%Ru-$Ni_{0.5}/Mg_{2.5}(Al)O$; d) 0.1 wt%Ru-$Ni_{0.5}/Mg_{2.5}(Al)O$; e) 0.5 wt%Ru-$Ni_{0.5}/Mg_{2.5}(Al)O$

full line, fresh sample; dotted line, sample after the reduction with H_2/N_2 (5/10 ml min^{-1}) at 900 ºC for 1 h, followed by the oxidation with O_2/N_2 (18.7/71.3 ml min^{-1}) at 700 ºC for 1 h.

Fig. 9 H_2 consumption in the TPR of supported Ru-Ni catalysts.

○, H_2 consumption on the fresh sample between 800 ºC and 900 ºC; ■, 1st H_2 consumption by the 1st peak around 550 ºC on the sample after the H_2/O_2 treatment; ●, 2nd H_2 consumption by the 2nd peak around 750 ºC on the sample after the H_2/O_2 treatment; □, Summation of the H_2 consumptions by the 1st and the 2nd peaks.

Figure 1. K. Takehira et al.

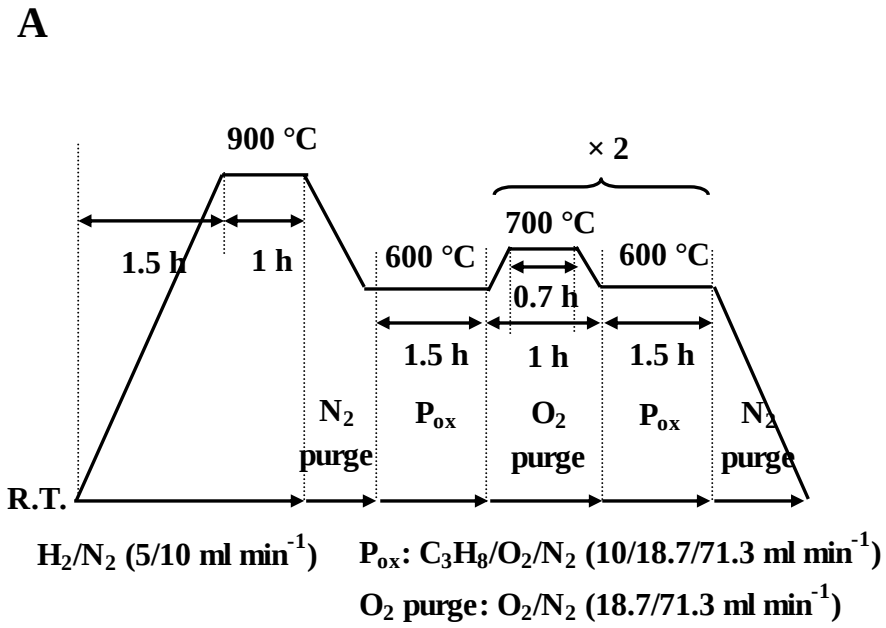

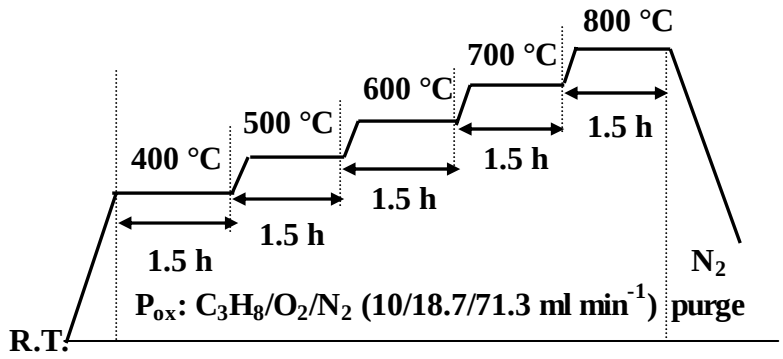

Figure 2. K. Takehira et al.

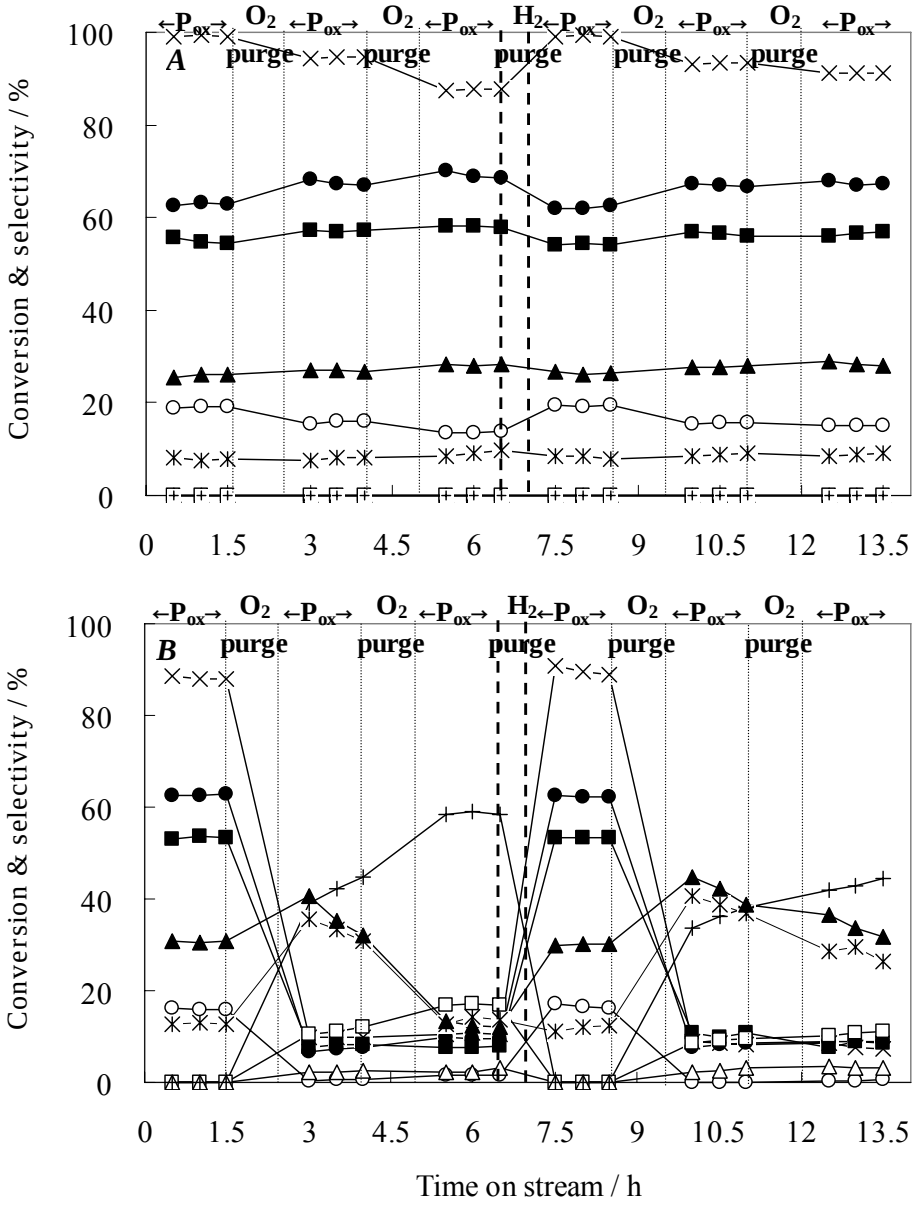

Figure 3. K. Takehira et al.

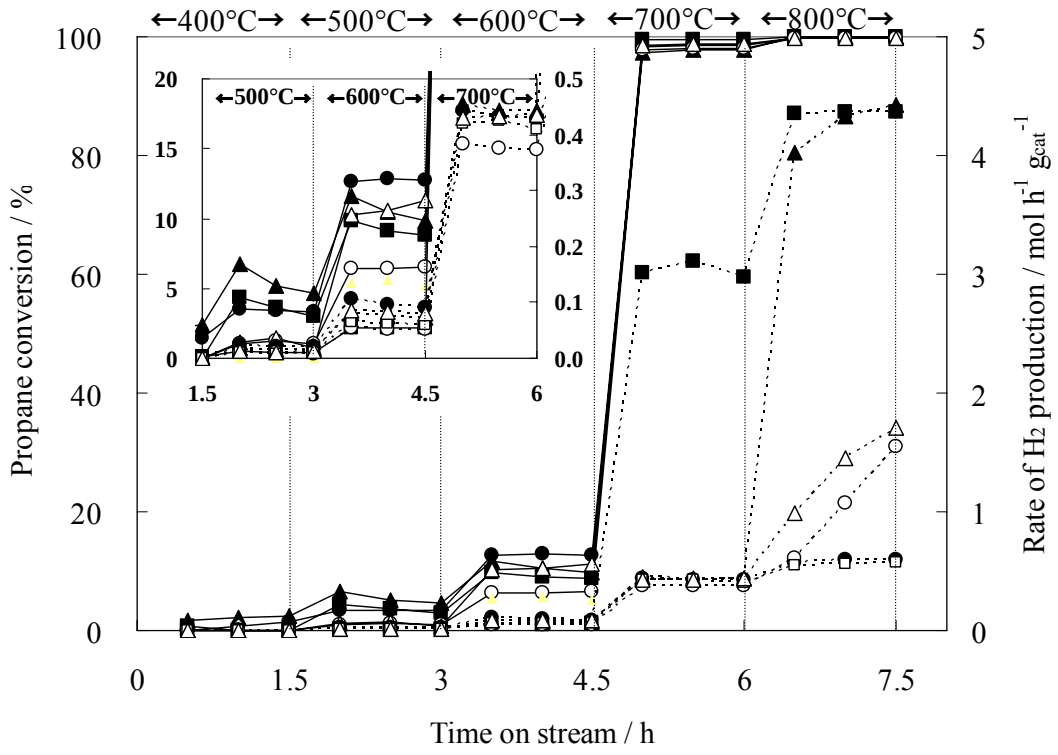

Figure 4. K. Takehira et al.

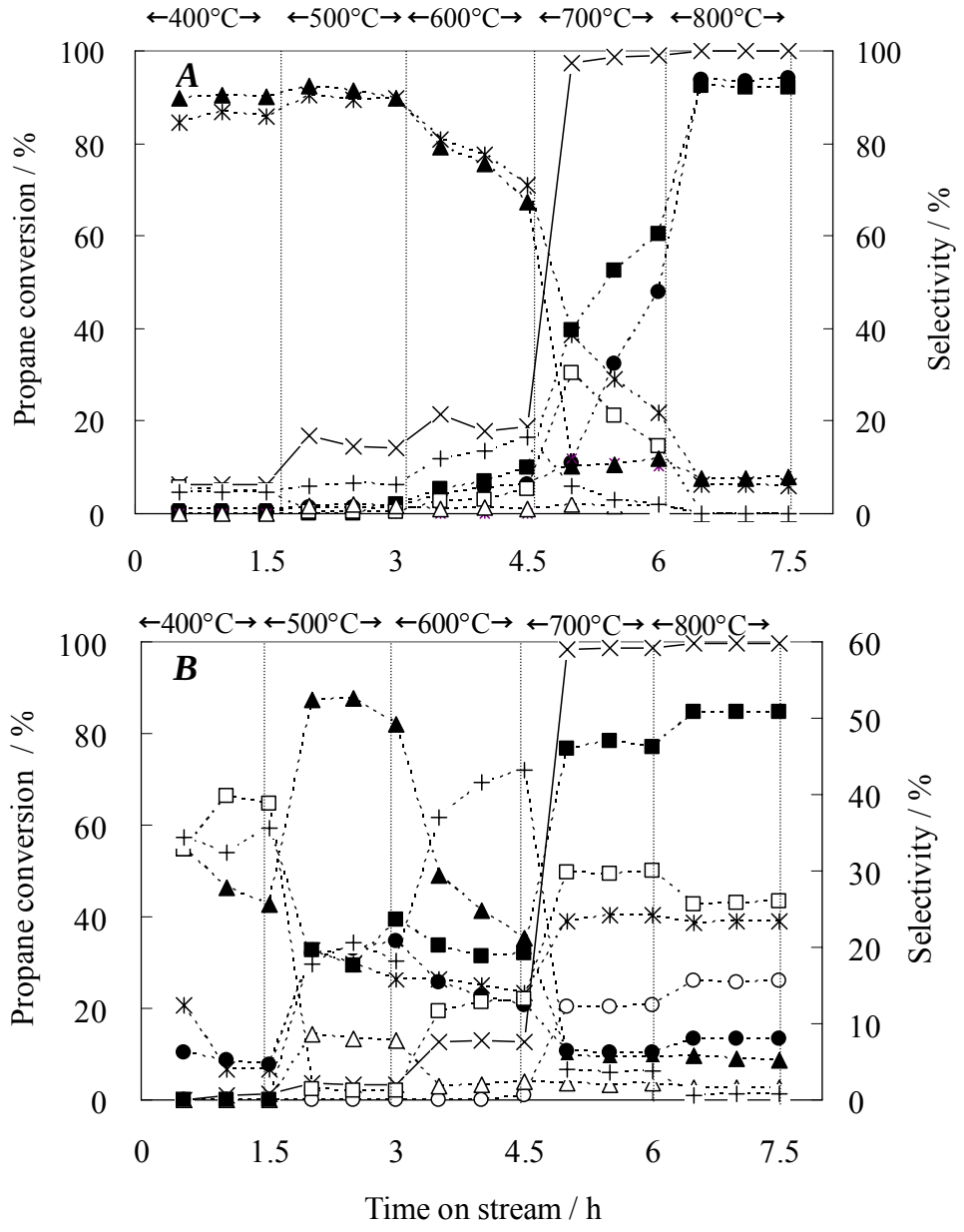

Figure 5. K. Takehira et al.

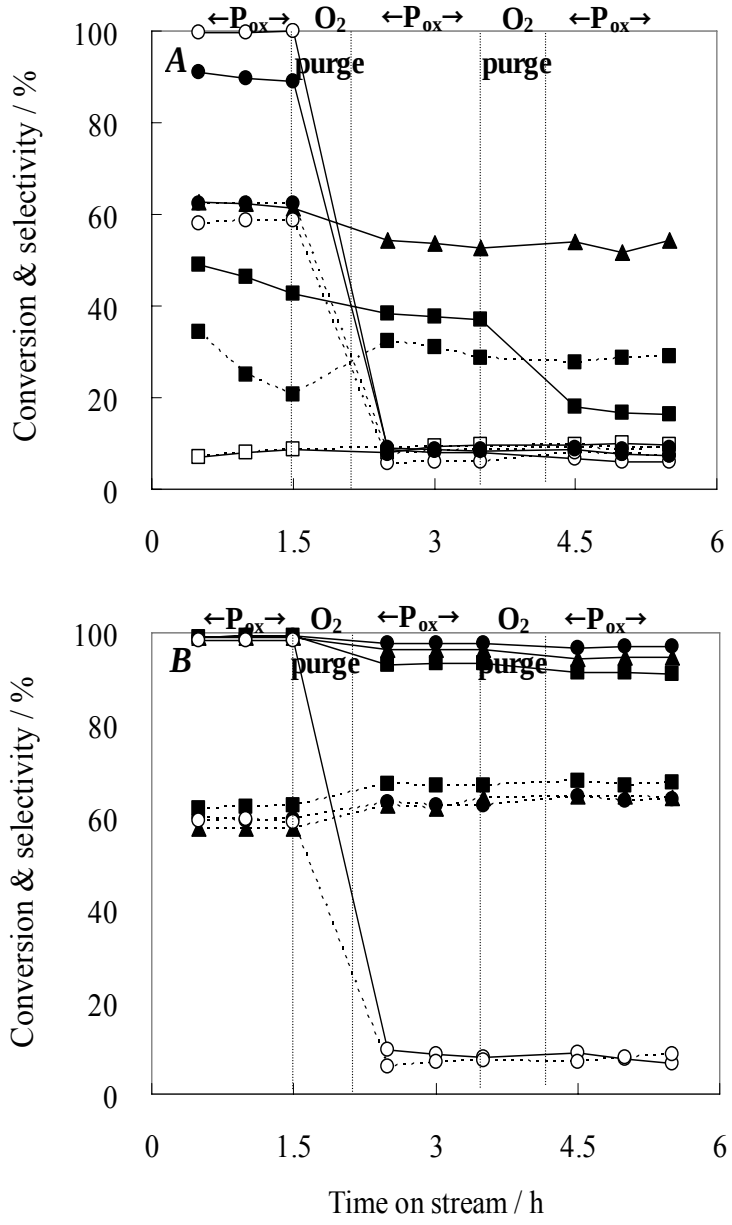

Figure 6. K. Takehira et al.

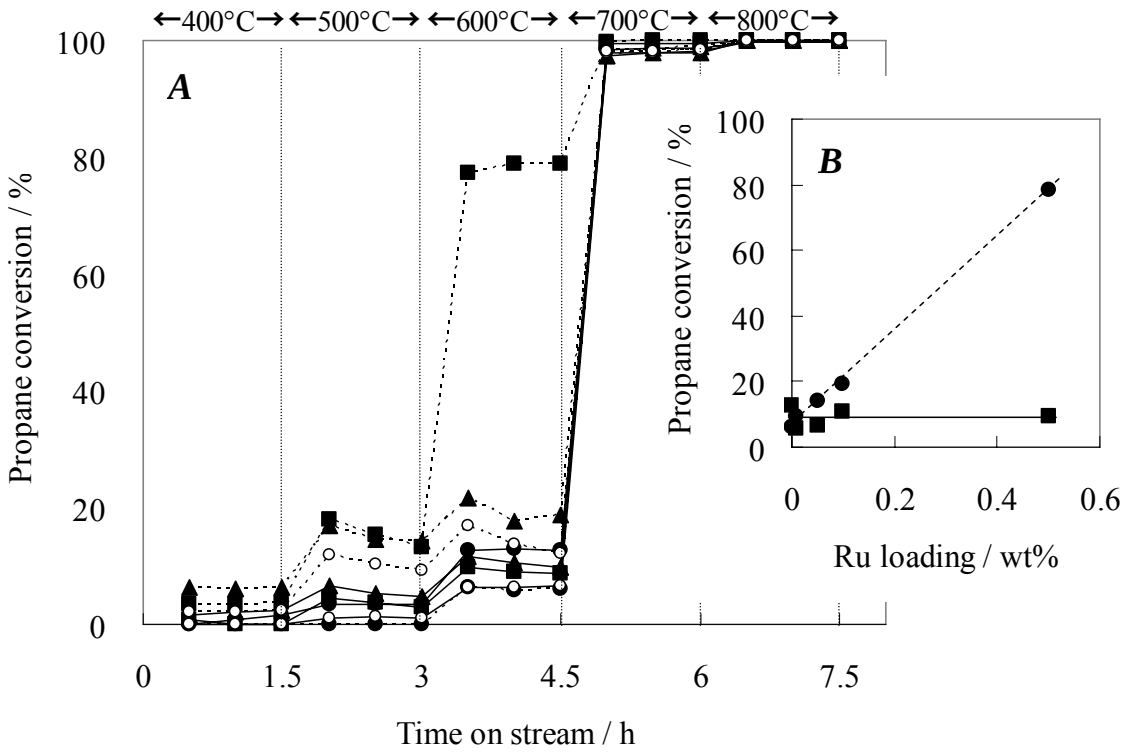

Figure 7. K. Takehira et al.

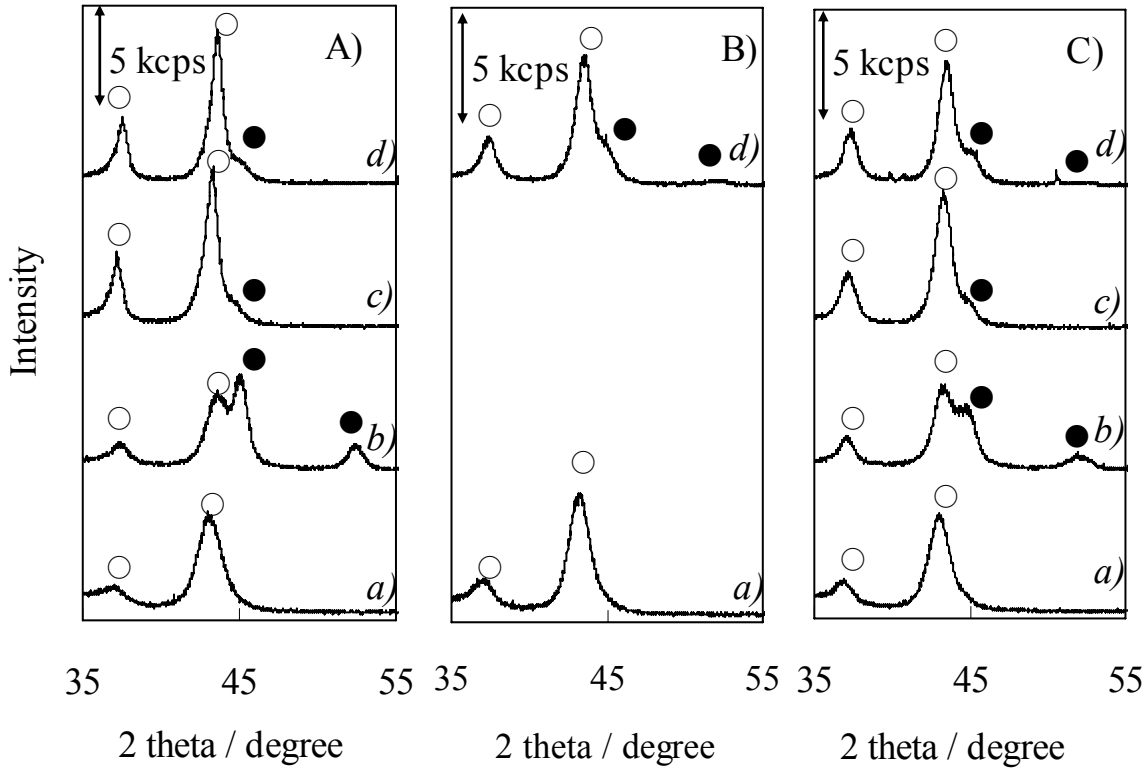

Figure 8. K. Takehira et al.

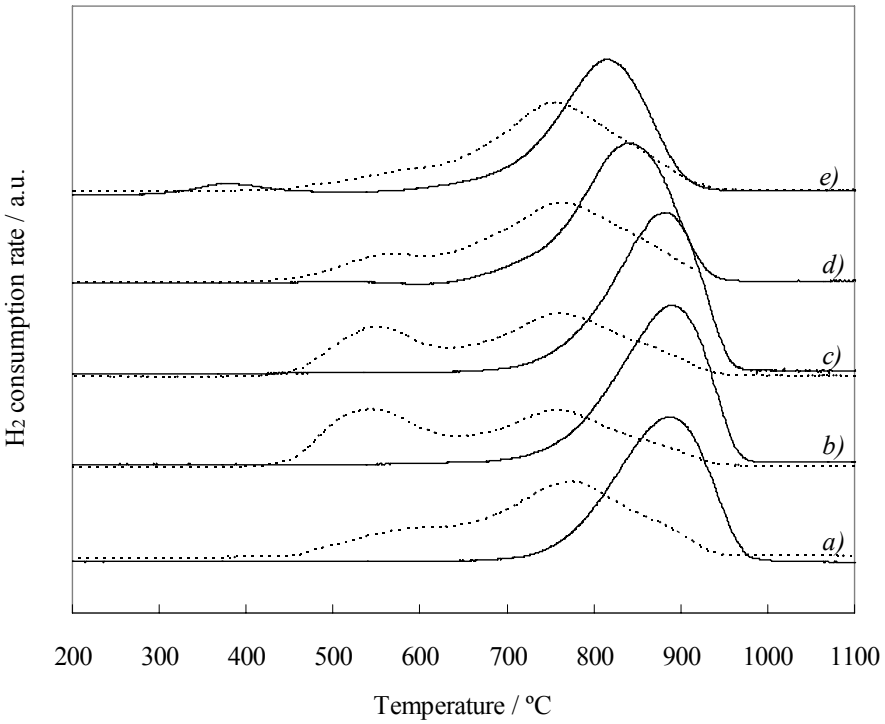

Figure 9. K. Takehira et al.